NIH Public Access
Author Manuscript
Anal Chem. Author manuscript; available in PMC 2010 March 15.

Published in final edited form as:
Anal Chem. 2009 March 15; 81(6): 2294–2302. doi:10.1021/ac802466g.

A Hybrid Capillary-Microfluidic Device for the Separation, Lysis, and Electrochemical Detection of Vesicles

Donna M. Omiatek[a], **Michael F. Santillo**[a], **Michael L Heien**[a], and **Andrew G. Ewing**[a,b,*]

a *Department of Chemistry, The Pennsylvania State University, University Park, PA 16802, USA*

b *Department of Chemistry, Göteborg University, Kemivägen 10, SE-41296 Göteborg, Sweden*

Abstract

The primary method for neuronal communication involves the extracellular release of small molecules that are packaged in secretory vesicles. We have developed a platform to separate, lyse, and electrochemically measure the contents of single vesicles using a hybrid capillary-microfluidic device. This device incorporates a sheath-flow design at the outlet of the capillary for chemical lysis of vesicles and subsequent electrochemical detection. The effect of sheath-flow on analyte dispersion was characterized using confocal fluorescence microscopy and electrochemical detection. At increased flow rates, dispersion was minimized, leading to higher separation efficiencies, but lower detected amounts. Large unilamellar vesicles (diameter ~ 200 nm), a model for secretory vesicles, were prepared by extrusion and loaded with an electroactive molecule. They were then separated and detected using the hybrid capillary-microfluidic device. Determination of size from internalized analyte concentration provides a method to characterize the liposomal suspension. These results were compared to an orthogonal size measurement using dynamic light scattering to validate the detection platform.

INTRODUCTION

Neurons communicate with each other via the release of small molecules that are packaged intracellularly in synaptic vesicles. These molecules are known to affect both the functional and behavioral aspects of an organism. Electrochemical measurements have quantified the amount of neurotransmitter released from synaptic vesicles at single cells during exocytosis.[1-15] By positioning a carbon-fiber microelectrode on a cell, the mole amount of electroactive neurotransmitter released can be quantified from current transients observed on the resultant amperometric trace using Faraday's Law (Q = nNF). Each transient is said to arise from a single release event. Much work has focused on the analysis of amperometric traces obtained from single cell electrochemistry experiments in order to better elucidate the mechanism of exocytotic release.[7, 8, 14]

An understanding of vesicle size and volume is an important parameter in the investigation of communication between cells. We have previously used electron microscopy and electrochemistry to characterize both the size of synaptic vesicles and the amount of neurotransmitter they contain from control cells and cells that have been manipulated to augment vesicular quantal size.[1, 2, 4-6, 16] From these experiments, frequency histograms have been used to link the size of vesicles to the mole amount of neurotransmitter housed within. While the amount released has been quantified, it is unclear whether the entire vesicular content is released during exocytosis. Therefore, development of an orthogonal method to

* To whom correspondence should be addressed: E mail: andrew.ewing@chem.gu.se Tel.: +46 31 772 2287 Fax: +1 814 863 8081.

NIH-PA Author Manuscript
NIH-PA Author Manuscript
NIH-PA Author Manuscript

NIH-PA Author Manuscript

NIH-PA Author Manuscript

NIH-PA Author Manuscript

analyze neurotransmitter content in single synaptic vesicles isolated from the cellular environment is necessary.

Capillary electrophoresis (CE) can be used for the separation and isolation of individual micro- and sub-micrometer size particles, including sub-cellular components.[17-25] We have developed a platform that takes advantage of the separation capabilities of CE to isolate and electrochemically measure the contents of single vesicles. The system presented here was designed to separate vesicles by an electric field in a fused-silica capillary that terminates onto a PDMS-based microfluidic device. As vesicles exit the separation capillary, the microfluidic device provides an interface for the chemical lysis of the membrane and subsequent electrochemical detection of the vesicle contents. Lysis buffer is delivered to the detection zone in a sheath-flow format, with a carbon-fiber microelectrode positioned in the analyte flow stream, similar to previous electrochemical sheath-flow devices.[26] The effect of sheath-flow on electrochemical detection was characterized using catechol solutions, and then individual large unilamellar vesicles (LUVs) loaded with dopamine (DA) were detected using the device. Liposomes are a model for synaptic vesicles; they can be synthesized to be structurally similar to vesicles and can be loaded with analyte. The detection scheme presented here is well suited for the analysis of synaptic vesicles; the redox nature of various neurotransmitters requires no external label and the corresponding amount of neurotransmitter can be directly quantified from isolated vesicles.

EXPERIMENTAL SECTION

Reagents

Catechol (CAT), 3-hydroxytyramine hydrochloride (DA), *N*-tris(hydroxymethyl)methyl-2-aminoethanesulfonic acid (TES), sodium hydroxide, sodium dodecyl sulfate (SDS), fluorescein isothiocyanate (FITC), rhodamine B, and hydrodfluoric acid (aq. 48%) were obtained from Sigma Aldrich (St. Louis, MO). All chemicals were used as received. The separation buffer consisted of 50 mM TES with 2% 1-propanol, and the lysis buffer was 50 mM TES with 5% (w/v) SDS. Buffers were adjusted to pH 7.4 using NaOH, filtered through 0.2 μm pore size filters (Nalgene, Rochester, NY), and purged with Ar (*g*) for 30 min prior to use to minimize oxidation of electroactive analyte. Standard solutions of CAT and DA were prepared as 10 mM stock solutions in separation buffer and diluted to the desired concentrations.

Liposome Preparation

Cholesterol (ovine wool) was obtained as a powder and 1,2-dipalmitoyl-*sn*-glycero-3-phosphocholine (DPPC) was obtained as a 50 mg/mL solution dissolved in chloroform (Avanti Polar Lipids, Inc., Alabaster, AL). Cholesterol powder was dissolved in chloroform to yield a 10 mg/mL stock solution. DPPC: cholesterol liposomes (80:20 mole ratio) were prepared using a modified technique provided by the distributor to yield large unilamellar vesicles by extrusion (LUVET).[27] Briefly, aliquots of DPPC (46 μL) and cholesterol (16 μL) were combined with 138 μL of chloroform and evaporated for 4 h. Following this, 5 mL of 150 mM DA in rehydrating buffer (50 mM TES, pH 7.4) was added to yield a final lipid concentration of 0.34 mg/mL. DA was excluded from the rehydrating solution for control liposome preparation. The lipid mixture was left to hydrate in the DA-containing buffer for 30 min. After this time period, the flask containing the mixture was subjected to five freeze/thaw cycles to promote entrapment of water-soluble compounds into the liposomes.[28] This was accomplished by alternating the flask between a dry ice/acetone and warm water bath. The mixture was then extruded through a 0.2 μm polycarbonate membrane for a total of twenty passes (Mini Extruder Kit, Avanti Polar Lipids, Inc., Alabaster, AL) to yield a monodisperse suspension of unilamellar liposomes.

NIH-PA Author Manuscript

NIH-PA Author Manuscript

NIH-PA Author Manuscript

Excess DA was removed from the liposome suspension by washing with a 10,000 MW dialysis cassette in DI water for 2 h (Slide-A-Lyzer, Thermo Scientific, Rockford, IL).

Microfluidic Device Fabrication

Microfluidic channels were fabricated using standard photo- and soft- lithography methods. A photolithographic mask made from a high resolution laser photoplot (CAD/ Art Services, Inc., Bandon, OR) was printed with the device features. A master mold was developed by spin-coating 125 μm of SU-8 100 negative photoresist (MicroChem Corp., Newton, MA) on a 3 inch silicon wafer (Silicon Quest International, Inc., Santa Clara, CA). The mask was then placed over the wafer, exposed to ultraviolet light, and developed according to the resist manufacturer protocol.

Soft lithography was carried out using a Sylgard® 184 silicone elastomer kit (Dow Corning Corp., Midland, MI). A 10:1 ratio of poly(dimethylsiloxane) (PDMS) prepolymer base to curing agent was cast onto the master mold and cured at 70 °C for 2 h. The PDMS layer was then peeled from the master, revealing an impression of microfluidic channels. The center channel served to secure the separation capillary in the finished hybrid device. The other two channels, each 200 μm wide, are set at a 30 ° angle to the center channel and used to direct lysis buffer to the capillary outlet in a sheath-flow format. The three channels converge into a 650 μm wide channel where the electrode is placed for detection. A buffer reservoir for capillary electrophoresis was cut into a 2 mm layer of PDMS and plasma-bonded to a 75 × 50 mm glass micro slide (Corning Inc., Corning, NY). The layer containing imprinted microfluidic channels was then exposed to oxygen plasma and bonded onto the reservoir layer to form the three-layer hybrid device (100 W, 1 min.).

Separations

Fused-silica capillaries (15 μm i.d./150 μm o.d., Polymicro Technologies, Phoenix, AZ) were filled with separation buffer using a stainless steel reservoir with applied He pressure (400 psi). Electrokinetic injections were performed for 5 or 20 s at 5 kV and separations were carried out at 15 kV (333 V/cm) using a high voltage supply (Spellman, Hauppauge, NY). Capillaries were conditioned before each separation by rinsing at 15 kV with 1 M NaOH for 2 min, Ultratrol™ Dynamic Pre-Coat-HN (Target Discovery, Palo Alto, CA) for 5 min, and separation buffer for 10 min. Lysis solution was continuously flowed through the microchannels during separations at a volumetric rate of 0.5μL/min unless otherwise noted.

Capillaries were prepared for electrochemical detection by removing 2 mm of the polyimide coating with a flame and subsequently etching the exposed fused-silica by purging He (250 psi) for 15 min in an HF bath. This resulted in an etch with a frustum geometry measuring approximately 40 μm wide at the base, which serves to both ease placement of the electrode at the capillary outlet, as well as to decouple the applied separation voltage from the electrochemical cell.[29]

Capillary Electrophoresis with Electrochemical Detection (CE-ECD) on the Hybrid Platform

A CE system with end-column amperometric detection was built in-house and used as previously described.[30] Modifications were made to the system to integrate hydrodynamic flow of lysis buffer into the detection zone. Briefly, 45 cm of capillary was threaded into the center channel of the microfluidic device. A syringe pump (KD Scientific, Holliston, MA) was used to control volumetric flow of lysis buffer via 1 mL plastic syringes. Polyethylene tubing (0.86 mm i.d./1.52 mm o.d., Becton Dickinson, Franklin Lakes, NJ) was fed through inlet holes to the microchannels. Amperometric electrochemical detection was carried out with a two-electrode format. A 5 μm-diameter carbon fiber was sealed in a glass capillary as previously described.[31] A cylindrical carbon-fiber electrode was cut to a length of approximately 500

NIH-PA Author Manuscript

NIH-PA Author Manuscript

NIH-PA Author Manuscript

μm from the glass seal. The electrode was held at 0.90 V versus a silver wire quasi-reference electrode (Ag QRE, 0.25 mm diameter, Alfa Aesar, Ward Hill, MA). The carbon-fiber electrode was positioned at the outlet of the capillary using an x,y,z- micromanipulator (Newport, Irvine, CA).

Current was measured using a Keithly model 427 (5 Hz bandpass) current amplifier (Cleveland, OH) and digitized at 100 Hz with a National Instruments PCI-6221 DAQ card using LabView 8.0 software (National Instruments, Austin, TX) written in house. OriginLab 8.0 (Northampton, MA) was used to generate electropherograms and Mini Analysis (Synaptosoft Inc., Fort Lee, NJ) was used for analysis of the resultant peaks to determine amplitude, area, and half-width. Events were counted if the signal was greater than three times the RMS baseline noise and the half-width was less than 100 ms.

Confocal Fluorescence Microscopy

Fluorescence images were acquired using a laser-scanning confocal microscope (Leica TCS SP5, Mannheim, Germany). To visualize fluid flow on the device, FITC solution (λ_{ex} 488 nm, λ_{em} 500−560 nm) was pumped through the microchannels and CE was carried out as described above. For the flow rate studies, rhodamine B (λ_{ex} 543 nm, λ_{em} 560−650 nm) in separation buffer was continuously injected into the capillary and run at 166 V/cm.

Simulations

Computational fluid dynamics (CFD) simulations were performed with Comsol Multiphysics 3.4 (Comsol, Inc., Burlington, MA), a finite element method solver. A two-dimensional geometry was used to model a top view of the capillary-microfluidic hybrid system. The following constants were used: diffusion coefficient, $D = 4.0 \times 10^{-6}$ cm^2/s; density, $\rho = 1.0$ g/cm^3; dynamic viscosity, $\eta = 1.0 \times 10^{-3}$ Pa s; initial bulk concentration, $c_0 = 100$ mM. Incompressible Navier-Stokes equations were initially solved, given by:

$$\frac{\partial \mathbf{u}}{\partial t} + \rho \mathbf{u} \cdot \nabla \mathbf{u} = -\nabla_p + \eta \nabla^2 \mathbf{u}$$
$$\nabla \cdot \mathbf{u} = 0$$

where **u** is velocity, t is time, ρ is density, p is pressure, and η is dynamic (absolute) viscosity. Subsequently, the convection/diffusion equation,

$$\frac{\partial c}{\partial t} + \mathbf{u} \cdot \nabla_c = D \nabla^2 c$$

was solved, where c is concentration, t is time, **u** is velocity, and D is the diffusion coefficient. The linear flow rate of solution exiting the capillary was fixed at 0.055 cm/s, and the velocity of sheath-flow was varied, yielding unique concentration profiles corresponding to each sheath-flow rate.

To model the detection of dopamine in a liposome, a one-dimensional finite-difference simulation was used. The in-house simulation program was written in LabView. Mass transport was considered diffusional and was described by Fick's second law, which for planar diffusion is:

$$\frac{d[DA]}{dt} = D \frac{d^2[DA]}{dx^2}$$

NIH-PA Author Manuscript

NIH-PA Author Manuscript

NIH-PA Author Manuscript

The dopamine concentration was initially set to zero, then the concentration in a liposome (assumed to be 150 mM) was introduced into spatial elements encompassing the experimentally measured diameter of a liposome (*vide infra*). The diffusion coefficient for dopamine (D) in this space was assumed to be 6×10^{-6} cm^2/s. Since amperometric measurements were performed, the concentration at the electrode surface was assumed to be zero as dopamine was oxidized to the ortho-quinone by the following reaction:

$$DA \rightarrow DOQ + 2H^+ + 2e^-$$

The determined flux is then converted to current by the following equation:

$$i = -nFAJ$$

Where n is the number of equivalents, F is Faraday's constant, J is the flux, and A is the area. To yield accurate current amplitudes, the electrode area was set so the sum of the resultant volume elements containing a total amount of dopamine equal to that in a liposome. The resultant current versus time curve was digitally filtered (5 Hz low pass, one pole) to match the bandpass of the current amplifier, and a 100 ms time epoch was analyzed to match the time window for experimental peaks.

Dynamic Light Scattering

A Zetasizer Nano S (Malvern Instruments, Worcestershire, UK) was used to acquire light scattering data. Measurements were collected using a 4 mW HeNe laser operated at 633 nm. Liposome suspensions were diluted 10-fold in 50 mM TES buffer. Data were collected in size mode at 25 °C and fit using instrument software.

RESULTS AND DISCUSSION

Microfluidic Device Fabrication

A hybrid capillary-microfluidic device is presented in this study for the separation, chemical lysis, and electrochemical detection of vesicles (Figure 1A). The device consists of two PDMS layers bonded onto a glass microscope slide. The top PDMS layer contains a microchannel to secure the separation capillary, which terminates into a buffer reservoir. Adjacent to it on either side are microchannels used to deliver solution in a sheath-flow format for the lysis of vesicles exiting the capillary. This top layer is bonded to a lower layer of PDMS containing a buffer reservoir where the electrical ground and reference electrode are placed. For the detection of redox active analyte, a cylindrical carbon-fiber microelectrode is positioned at the outlet of the separation capillary, parallel to the flow stream spanning 500 μm in length.

Bright field and confocal fluorescence micrographs of the assembled device are shown in Figure 1B. These figures illustrate both electrophoretic and hydrodynamic flow. The capillary was placed approximately 500 μm beyond convergence of the central and lysis channels in order to ensure laminar flow was present in the detection zone. A solution of rhodamine B (red) was continuously injected onto the separation capillary at 133 V/cm, while FITC solution (green) was concurrently pumped through the lysis channels at a volumetric flow rate of 0.5 μL/min. The detection electrode is not pictured in these images.

Confocal Fluorescence Microscopy of Flow in the Hybrid Device

Flow through the sheath microchannels affects analyte dispersion as it exits the separation capillary. An optimal flow rate would (1) confine the eluent to the diffusion layer of the detection electrode, and (2) allow ample time for interaction of the eluent with the electrode.

NIH-PA Author Manuscript

NIH-PA Author Manuscript

NIH-PA Author Manuscript

We investigated analyte dispersion with confocal fluorescence microscopy and CFD simulations. Rhodamine B solution was continuously flowed through the separation capillary at a fixed rate (166 V/cm), while the rate of lysis buffer through the sheath channels was varied (0.1, 0.5, and 2 μL/min). The normalized concentration profile for the simulated diffusion of rhodamine B exiting the separation capillary is shown at different flow rates (Figure 2, black trace), and confocal fluorescence microscopy data for the complementary experiment is shown in red.

Confocal fluorescence micrographs and CFD simulations allow visualization of the relationship between flow rate and the eluent concentration profile. Line scans were taken 50 Lm from the outlet perpendicular to the flow stream in both cases as indicated by the white arrows. As the flow rate is increased, the eluent is hydrodynamically focused, minimizing diffusional broadening in the detection zone. The experimental data matches that predicted by the CFD simulation. The correlation coefficient between the simulation and fluorescence data, r^2, was 0.99, 0.98, and 0.96 for the 0.1, 0.5 and 2 uL/min flow rates, respectively. This illustrates the importance of electrode position and flow rate selection for optimal detection in this platform. An electrode with a radius of 3 μm has a diffusion layer thickness of approximately 20 μm.[32] From examination of the simulation and fluorescence data in Figure 2, at 0.1 μL/min, the electrode diffusion layer does not encompass the eluent concentration profile. At 2.0 μL/min the diffusion layer encompasses the entire eluent concentration profile; however, this high flow rate limits the interaction time with the detector. Indeed, the calculated linear flow velocity in the channel is 0.082 cm/s, allowing only 0.6 s for the solution to interact with a 500 μm long electrode positioned at the capillary outlet. The intermediate flow rate investigated, 0.5 μL/min, allows approximately 2.4 seconds of interaction time and encompasses approximately 70% of the eluent concentration profile. Therefore this intermediate flow rate comes closer to satisfying the two requirements stated above, when compared to either extreme.

Electrochemical Detection on the Hybrid Device

Sheath-flow rate affected analyte dispersion and the interaction time with the detection electrode as determined from fluorescence experiments. We then quantitatively investigated how sheath-flow influences the amount of analyte detected and the separation efficiency using CE-ECD. A plug of 100 μM CAT solution was injected onto the capillary, and detected as the flow rate was varied. In these experiments, flow driven by the electric field (111 V/cm injection, 333 V/cm run potential) was fixed and the hydrodynamic flow rate of lysis buffer through the sheath microchannels was varied from 0 to 2.0 μL/min. Varying the flow rate of lysis solution affects the electrochemical detection of analyte, but not the elution time; elution times for CAT were uniform across the flow rates investigated. Figure 3A contains representative electropherograms without (black trace) and with sheath-flow present at various flow rates (colored traces). When sheath-flow is present, greater mole amounts of CAT are detected at lower flow rates, however, lower separation efficiencies are observed (Figure 3B). Lower flow rates allow more time for the eluent to interact with the electrode surface, resulting in higher coulometric efficiency for the detection of CAT. In contrast, higher flow rates minimize the interaction time with the electrode surface, resulting in lower coulometric efficiency for the detection of CAT, but sharper peaks. Results for the detected analyte from this CE-ECD experiment are listed in Table 1.

In order to efficiently lyse vesicles and detect their contents, the velocity of the lysis solution must be slow enough to allow time for the micelles in the SDS-buffered solution to interact with the vesicle membrane, but fast enough to direct analyte to the electrode surface where they are subsequently detected. To determine the optimal flow rate, the mole amount of CAT and the total number of theoretical plates was plotted against flow rate for the solution studies (Figure 3B). The rate of 0.5 μ/min through the sheath channels was chosen because it yields

NIH-PA Author Manuscript

NIH-PA Author Manuscript

NIH-PA Author Manuscript

the most efficient peak shape at high coulometric detection efficiency for the plug of CAT solution. This is in agreement with the fluorescence experiments, which predicted 0.5 μL/min as optimal for the detection criterion set.

Separation and Detection of Liposomes

Liposomes are often used as a model for the analysis of cellular and sub-cellular membrane-bound components[33, 34] as well as to characterize a number of analytical methods in the areas of separations.[18, 35-38] Arriaga and co-workers have investigated liposomes loaded with a fluorescent dye by CE.[18] They were able to determine the apparent radius of individual liposomes according to the signal that arose from the relative intensity of fluorophore inside. A similar approach is used in this paper to characterize our CE-ECD hybrid device; however, the liposomes investigated have been loaded with an electroactive molecule to directly quantify the amount of analyte after membrane lysis by use of electrochemical detection.

We used the hybrid capillary-microfluidic device to separate and detect DA-loaded liposomes using carbon-fiber amperometry. Liposome suspensions were electrokinetically injected at 111 V/cm for 20 s and run at 333 V/cm. As the liposomes eluted from the separation capillary, they were lysed by the use of SDS-containing buffer, and the contents loaded inside the membrane were subsequently detected at an electrode, which was positioned at the outlet of the separation capillary. A portion of a representative electropherogram for the separation and detection of these samples are in Figure 4. Prior to 1500 s, the concentration of free dopamine remaining in the liposome suspension causes the detector to overload, limiting quantification in this region of the electropherogram. To prevent possible electrode fouling, an oxidizing voltage is not applied to the electrode until this time point. Figure 4A shows the CE-ECD results for a suspension of liposomes loaded with 150 mM DA. Each spike in the electropherogram corresponds to a single liposome. Using the frequency of detected events, there is a 0.5% probability that two liposomes would give rise to a single peak at a given time point in the electropherogram (based on Poisson statistics, 50 ms time bins, 0.09 events/bin). Pictured to the right in Figure 4A is an expanded temporal view of individual events to illustrate the peak characteristics associated with liposome lysis and detection.

The liposome suspension from Figure 4A was diluted ten-fold and injected again under the same parameters. The resultant electropherogram is shown in Figure 4B and an expanded view is to the right. As expected, a smaller number of peaks are detected upon dilution of the original suspension (140 vs. 2670 events). Figure 4C represents a control suspension of liposomes prepared using the same method as those in Figures 4A and B, but rehydrated in buffer that excluded DA. Few peaks were observed (4 peaks). The control suspension lacks the redox molecule required for electrochemical detection; therefore these liposomes do not yield a signal in the CE ECD experiments upon lysis. The few events observed in the electropherogram are most likely due to minor mechanical perturbations of the electrode; upon close inspection the peaks do not possess characteristics observed in the traces obtained from liposomes loaded with DA (peak amplitude and half-width). This demonstrates that the amperometric peaks in the electropherograms of DA loaded liposomes are due to oxidation of the DA at the electrode and not an artifact of the detection scheme.

Determination of Liposome Size

Quantification of DA detected from each liposome by CE-ECD can be accomplished using Faraday's Law. By integrating the area under each peak, the mole amount of DA detected per liposome can be determined. Using the known concentration of analyte loaded into each liposome, the internalized volume of DA solution can then be calculated. The liposomes are assumed to be geometrically spherical; thus the internalized volume can be used to directly calculate the radius for each liposome. This simplistic calculation makes two assumptions: 1)

NIH-PA Author Manuscript

NIH-PA Author Manuscript

NIH-PA Author Manuscript

the encapsulation of DA is 100% efficient and 2) the entire contents of the vesicle are oxidized at the electrode after lysis. These assumptions are clearly imperfect; loading efficiencies are known to vary depending on liposome composition, size, lamellarity, and the solute investigated.[28, 39-45] The liposome preparation in this study was designed, however, to both maximize encapsulation efficiency and minimize leakage of DA out of the liposomes after synthesis. The phospholipid composition chosen used long-chain unsaturated lipid (DPPC) to maximize encapsulation and cholesterol to minimize leakage.[41] Despite this, the data clearly suggest that DA is not fully encapsulated or leaks out after formation of the liposomes.

The calculated radii for individual liposomes detected by CE-ECD on the hybrid capillary-microfluidic platform are plotted as a normalized frequency distribution histogram in Figure 5A. DLS was employed to independently measure the radius of the liposomes. DLS measures the diffusion of particles over time and relates this measurement to the hydrodynamic radius of the particle by the Stokes-Einstein equation.

$$r(H) = \frac{kT}{6\pi\eta D}$$

In this equation $\boldsymbol{k}$ is Boltzmann's constant, T is the absolute temperature, $\boldsymbol{\eta}$ is the viscosity of the medium, and D is the translational diffusion coefficient of the particle. By correlating the measured diffusion coefficients for a number of particles in a given time period, the hydrodynamic radius $\boldsymbol{r(H)}$ of a population of particles is solved for and plotted as a frequency curve (Figure 5B).

Table 2 lists the results tabulated for the CE-ECD and DLS analyses of liposome suspensions. The suspension was extruded through a 0.2-μm membrane, which should yield liposomes with a radius 100 nm or less. CE-ECD detection of the DA-loaded liposomes corresponded to zeptomole quantities of DA detected for each individual lysis event in the electropherogram. The calculated amounts translate to a mean radius of 80 ± 18 nm based on the measured internalized volume of the analyte for liposomes loaded with 150 mM DA. These measurements extrapolate to a limit-of-detection corresponding to a liposome with a radius of 10 nm (based on peak amplitude, area, and loaded DA concentration). The hydrodynamic radius as measured by DLS for the same suspension was 115 ± 36 nm. There is a statistically significant difference between the two measurements (Mann-Whitney test, $p < 0.01$). The difference in size measurements highlights the limitations in the assumptions regarding encapsulation efficiency and coulometric efficiency (*vide supra*). Indeed, the amount detected by CE-ECD in liposomes is 35 ± 20 % of the estimated amount in the liposomes (using DLS measurements for size and assuming 100% loading efficiency). This difference could be due to two factors; 1) reported encapsulation efficiencies for LUVs in this size range vary from 15 – 60%[42] and 2) our detection may not be 100% efficient. Interestingly, the measured difference in size can be accounted for entirely by encapsulation efficiency, suggesting our detection scheme is highly efficient.

Modeling the Electrochemical Signal from Liposome Lysis

Although the difference between the expected amount of DA in a liposome and the experimentally determined amount can be accounted for with non-ideal encapsulation efficiencies, the coulometric efficiency of the device can also contribute to this discrepancy. Here coulometric efficiency is defined as the ratio of the amount of electroactive species detected to the amount present in a liposome. Unfortunately, there is no satisfactory standard to calibrate the device in order to determine coulometric efficiency of electroactive species released from membrane-bound components upon lysis. To approximate the coulometric efficiency of the device, we modeled the resultant electrochemical signal measured upon

NIH-PA Author Manuscript

NIH-PA Author Manuscript

NIH-PA Author Manuscript

liposome lysis and subsequent detection. In this explicit finite-difference simulation, liposomes were lysed a certain distance from the electrode, releasing their contents instantaneously, and the resultant flux of analyte at the electrode was determined as a function of time, converted to current, and filtered to allow direct comparison to experimental data. The shape of the resultant current versus time curves, particularly the half-width, was used to compare the simulation to experimental data.

The total flux at the electrode can be compared to the total amount of analyte originally in the liposome to yield the coulometric efficiency. The distance away from the electrode where the lysis occurs was varied to yield curves detailing how half-width and coulometric efficiency change as a function of distance (Figure 6). As the distance from the electrode decreases, the coulometric efficiency increases. The experimental data in Table 2 show the half-width for the measured liposomes as 42.2 ± 17.4 ms, which in the simulated data, corresponds to a liposome lysing approximately 0.25 μm away from the electrode, yielding a coulometric efficiency of 87%. Using the temporal profile of the amperometric events, the model suggests the liposomes are lysing in a region close to the electrode (< 2 μm), corresponding to coulometric efficiencies ranging from 70 − 90%. Interestingly, liposomes at a distance of more than 5 μm away would not cross the signal-to-noise threshold for detection (~0.3 pA), resulting in a lower coulometric efficiency at 48%. Furthermore, liposomes at this distance have large half-widths (98 ms) not observed in the experimental data. If a coulometric efficiency of 87% is applied to experimental data for the quantification of *individual* DA liposomes in this study, the encapsulation efficiency is 41 ± 22 %, which is in agreement with the expected range for bulk analyses reported in the literature.[42] Therefore, the hybrid microfluidic-CE-ECD platform described in this paper appears to be a valid tool for the lysis and subsequent detection of individual vesicles.

CONCLUSION

A hybrid capillary-microfluidic device has been fabricated for the separation of vesicles that are chemically lysed and subsequently detected using end-column carbon-fiber amperometry. Sheath-flow of lysis buffer integrated onto the device minimized the diffusional broadening of eluent in the detection zone as determined by confocal fluorescence microscopy and electrochemistry. Liposomes, a model for synaptic vesicles, were injected onto the capillary for separation, lysis, and detection of their contents. The electropherograms from diluted liposome suspensions and from the control liposomes possessed less peaks, confirming the selectivity of the detection scheme. DA vesicle size was estimated by electrochemically measuring the amount of internalized analyte and relating this to the volume. The vesicle size determination from these experiments differed from those obtained by DLS measurements, which describes the hydrodynamic radius of particles in the biocolloidal suspension. This variation can be attributed to non-ideal encapsulation efficiency. These data support the contention that the characterized hybrid capillary-microfluidic device can be used to investigate the amount of neurotransmitter present in individual synaptic vesicles isolated from the cell environment.

ACKNOWLEDGEMENTS

The authors thank Dr. Raafat Malek of Penn State's Materials Characterization Laboratory for assistance in interpreting DLS data. This work was supported by the NIH grant 5R01EB00352−10. A.G.E. is supported by a Marie Curie Chair from the European Union's 6th Framework. This publication was supported by The Pennsylvania State University Materials Research Institute Nano Fabrication Network and the National Science Foundation Cooperative Agreement No. 0335765, National Nanotechnology Infrastructure Network, with Cornell University.

REFERENCES

1. Anderson BB, Chen G, Gutman DA, Ewing AG. Brain Res 1998;788:294–301. [PubMed: 9555063]

NIH-PA Author Manuscript

NIH-PA Author Manuscript

NIH-PA Author Manuscript

2. Anderson BB, Chen G, Gutman DA, Ewing AG. J. Neurosci. Methods 1999;88:153–161. [PubMed: 10389661]
3. Anderson BB, Ewing AG, Sulzer D. Methods Enzymol 1998;296:675–689. [PubMed: 9779482]
4. Anderson BB, Zerby SE, Ewing AG. J. Neurosci. Methods 1999;88:163–170. [PubMed: 10389662]
5. Colliver TL, Hess EJ, Pothos EN, Sulzer D, Ewing AG. J. Neurochem 2000;74:1086–1097. [PubMed: 10693940]
6. Colliver TL, Pyott SJ, Achalabun M, Ewing AG. J. Neurosci 2000;20:5276–5282. [PubMed: 10884311]
7. Amatore C, Arbault S, Bonifas I, Bouret Y, Erard M, Ewing AG, Sombers LA. Biophys. J 2005;88:4411–4420. [PubMed: 15792983]
8. Amatore C, Arbault S, Bonifas I, Guille M, Lemaitre F, Verchier Y. Biophys. Chem 2007;129:181–189. [PubMed: 17587484]
9. Kozminski KD, Gutman DA, Davila V, Sulzer D, Ewing AG. Anal. Chem 1998;70:3123–3130. [PubMed: 11013717]
10. Mosharov EV, Sulzer D. Nat. Methods 2005;2:651–658. [PubMed: 16118635]
11. Pothos EN, Davila V, Sulzer D. J. Neurosci 1998;18:4106–4118. [PubMed: 9592091]
12. Pothos EN, Larsen KE, Krantz DE, Liu Y, Haycock JW, Setlik W, Gershon MD, Edwards RH, Sulzer D. J. Neurosci 2000;20:7297–7306. [PubMed: 11007887]
13. Staal RG, Mosharov EV, Sulzer D. Nat. Neurosci 2004;7:341–346. [PubMed: 14990933]
14. Sulzer D, Edwards R. Neuron 2000;28:5–7. [PubMed: 11086975]
15. Wightman RM, Jankowski JA, Kennedy RT, Kawagoe KT, Schroeder TJ, Leszczyszyn DJ, Near JA, Diliberto EJ, Viveros OH. Proc. Natl. Acad. Sci. USA 1991;88:10754–10758. [PubMed: 1961743]
16. Sombers LA, Hanchar HJ, Colliver TL, Wittenberg N, Cans A, Arbault S, Amatore C, Ewing AG. J. Neurosci 2004;24:303–309. [PubMed: 14724228]
17. Chen Y, Xiong G, Arriaga EA. Electrophoresis 2007;28:2406–2415. [PubMed: 17577888]
18. Duffy CF, Gafoor S, Richards DP, Admadzadeh H, O'Kennedy R, Arriaga EA. Anal. Chem 2001;73:1855–1861. [PubMed: 11338602]
19. Duffy CF, McEathron AA, Arriaga EA. Electrophoresis 2002;23:2040–2047. [PubMed: 12210257]
20. Fuller KM, Arriaga EA. Anal. Chem 2003;75:2123–2130. [PubMed: 12720351]
21. Gunasekera N, Olson KJ, Musier-Forsyth K, Arriaga EA. Anal. Chem 2004;76:655–662. [PubMed: 14750860]
22. Johnson RD, Navratil M, Poe BG, Xiong G, Olson KJ, Ahmadzadeh H, Andreyev D, Duffy CF, Arriaga EA. Anal. Bioanal. Chem 2007;387:107–118. [PubMed: 16937092]
23. Kostal V, Arriaga EA. Electrophoresis 2008;29:2578–2586. [PubMed: 18576409]
24. Whiting CE, Arriaga EA. Electrophoresis 2006;27:4523–4531. [PubMed: 17117462]
25. Whiting CE, Arriaga EA. J. Chromatogr. A 2007;1157:446–453. [PubMed: 17521658]
26. Ertl P, Emrich CA, Singhal P, Mathies RA. Anal. Chem 2004;76:3749–3755. [PubMed: 15228350]
27. 2008. www.avantilipids.com/PreparationOfLiposomes.htm, A. P. L. I.
28. Mayer LD, Hope MJ, Cullis PR, Janoff AS. Biochim. Biophys. Acta 1985;817:193–196. [PubMed: 4005257]
29. Woods LA, Ewing AG. Chemphyschem 2003;4:207–211. [PubMed: 12619421]
30. Powell PR, Woods LA, Ewing AG. J. Sep. Sci 2005;28:2540–2545. [PubMed: 16405186]
31. Kawagoe KT, Zimmerman JB, Wightman RM. J. of Neurosci. Methods 1993;48:225–240. [PubMed: 8412305]
32. Bard, AJF.; L. R., editors. Electrochemical Methods. John Wiley and Sons; New York: 1980.
33. Cans AS, Wittenberg N, Eves D, Karlsson R, Karlsson A, Orwar O, Ewing A. Anal. Chem 2003;75:4168–4175. [PubMed: 14632131]
34. Cans AS, Wittenberg N, Karlsson R, Sombers L, Karlsson M, Orwar O, Ewing A. Proc. Natl. Acad. Sci. USA 2003;100:400–404. [PubMed: 12514323]
35. Radko SP, Stastna M, Chrambach A. Anal. Chem 2000;72:5955–5960. [PubMed: 11140762]

NIH-PA Author Manuscript

NIH-PA Author Manuscript

NIH-PA Author Manuscript

36. Radko SP, Stastna M, Chrambach A. J. Chromatogr. B Biomed. Sci. Appl 2001;761:69–75. [PubMed: 11585133]
37. Pysher MD, Hayes MA. Langmuir 2004;20:4369–4375. [PubMed: 15969140]
38. Pysher MD, Hayes MA. Langmuir 2005;21:3572–3577. [PubMed: 15807603]
39. Dominak LM, Keating CD. Langmuir 2007;23:7148–7154. [PubMed: 17516666]
40. Lohse B, Bolinger P-Y, Stamou D. J. Am. Chem. Soc 2008;130:14372–14373. [PubMed: 18842043]
41. Manojlovic V, Winkler K, Bunjes V, Neub A, Schubert R, Bugarski B, Leneweit G. Colloid. Surface B 2008;64:284–296.
42. Mayer LD, Bally MB, Hope MJ, Cullis PR. Chem. Phys. Lipids 1986;40:333–345. [PubMed: 3742676]
43. Mayer LD, Tai LC, Ko DS, Masin D, Ginsberg RS, Cullis PR, Bally MB. Cancer Res 1989;49:5922–5930. [PubMed: 2790807]
44. Sun B, Chiu DT. Anal. Chem 2005;77:2770–2776. [PubMed: 15859592]
45. Lian T, Ho RJY. J. Pharm. Sci 2001;90:667–680. [PubMed: 11357170]

NIH-PA Author Manuscript
NIH-PA Author Manuscript
NIH-PA Author Manuscript

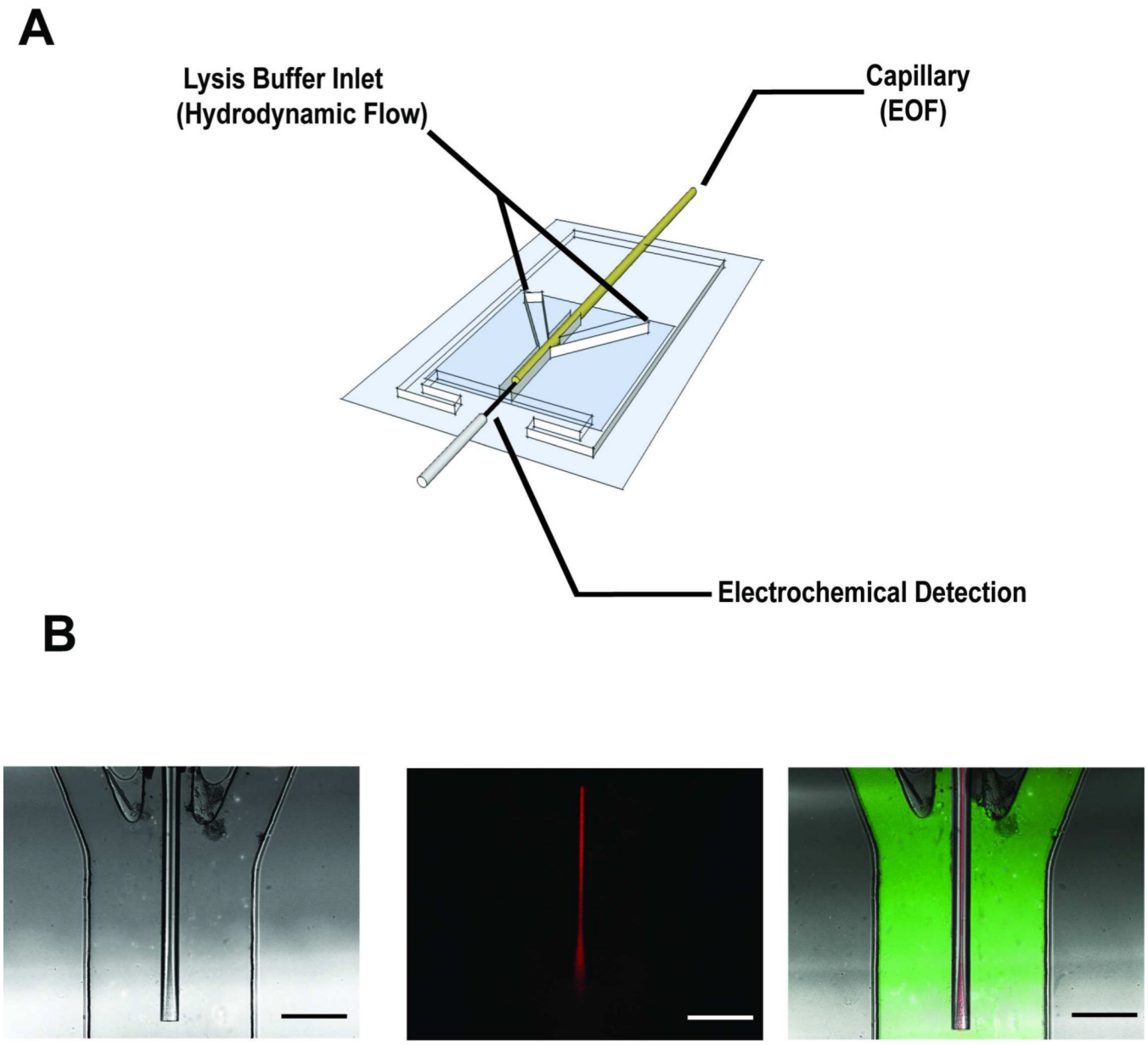

Figure 1.

Three layer PDMS device for the end-column lysis and electrochemical detection of vesicles separated by capillary electrophoresis. (A) Schematic of device (not drawn to scale). Three 200 μm × 125 μm channels converge into a 650 μm × 125 μm channel where contents exiting the capillary are lysed and detected at a carbon-fiber microelectrode. (B) Bright field and confocal fluorescence images of the device. A continuous injection 100 μM rhodamine B solution (red) is flowed through the capillary using electroosmotic flow (166 V/cm) and 36 μM FITC solution (green) is flowed through the lysis channels using hydrodynamic flow controlled by a syringe pump (0.5 μ/min, scale bar = 200 μm).

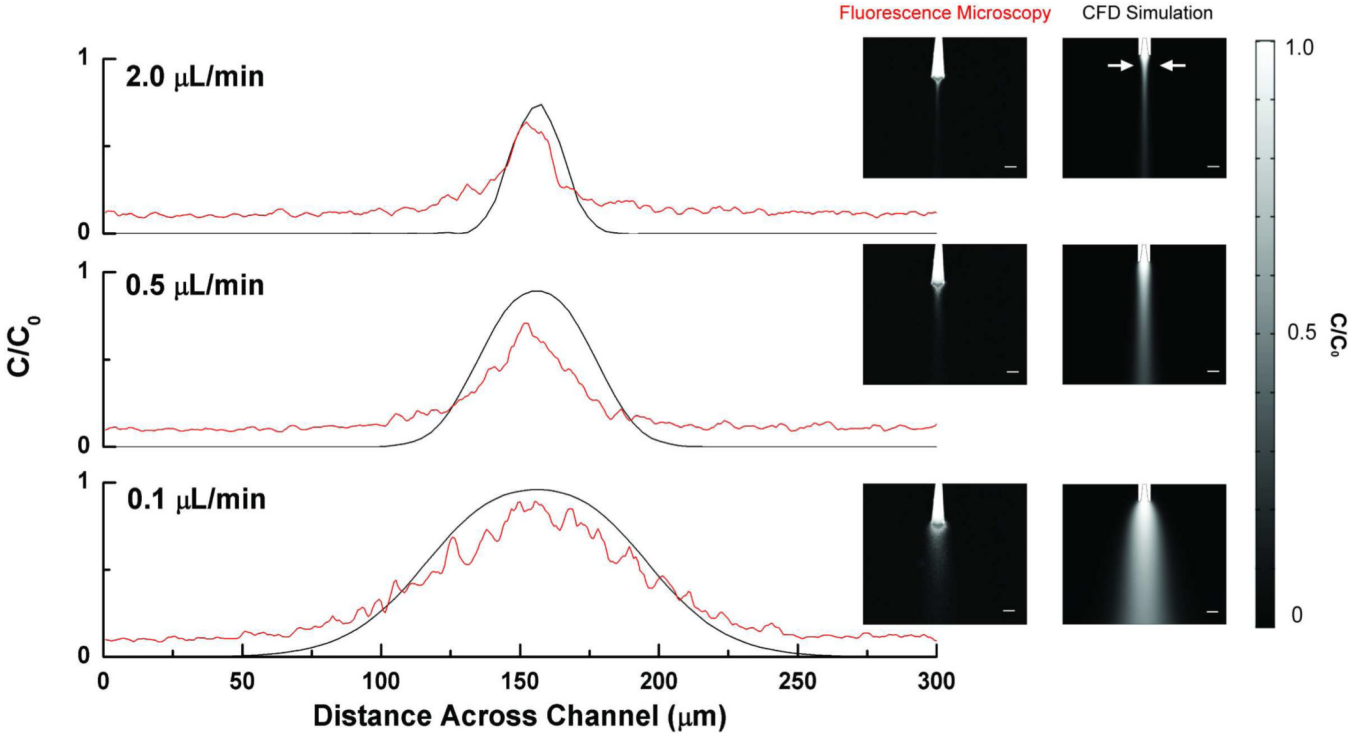

Figure 2.

Effect of volumetric flow rate through lysis channels on the fluorescence detection of analyte. A continuous injection of 100 μM rhodamine B solution was flowed through the capillary using electroosmotic flow (166 V/cm). Volumetric flow rates of buffer through the lysis channels were varied. Data are line scans taken perpendicular to the flow stream, 50 μm from the outlet as shown by the white arrows. Fluorescence measurements are indicated by the red trace and CFD measurements by the black trace. Confocal fluorescence microscopy images and CFD simulations for diffusion of separation eluent at 0.1, 0.5, and 2 μL/min are pictured to the right of the line scan traces (Scale bar = 50 μm). Fluorescence data was smoothed using a moving average of five points.

NIH-PA Author Manuscript
NIH-PA Author Manuscript
NIH-PA Author Manuscript

NIH-PA Author Manuscript
NIH-PA Author Manuscript
NIH-PA Author Manuscript

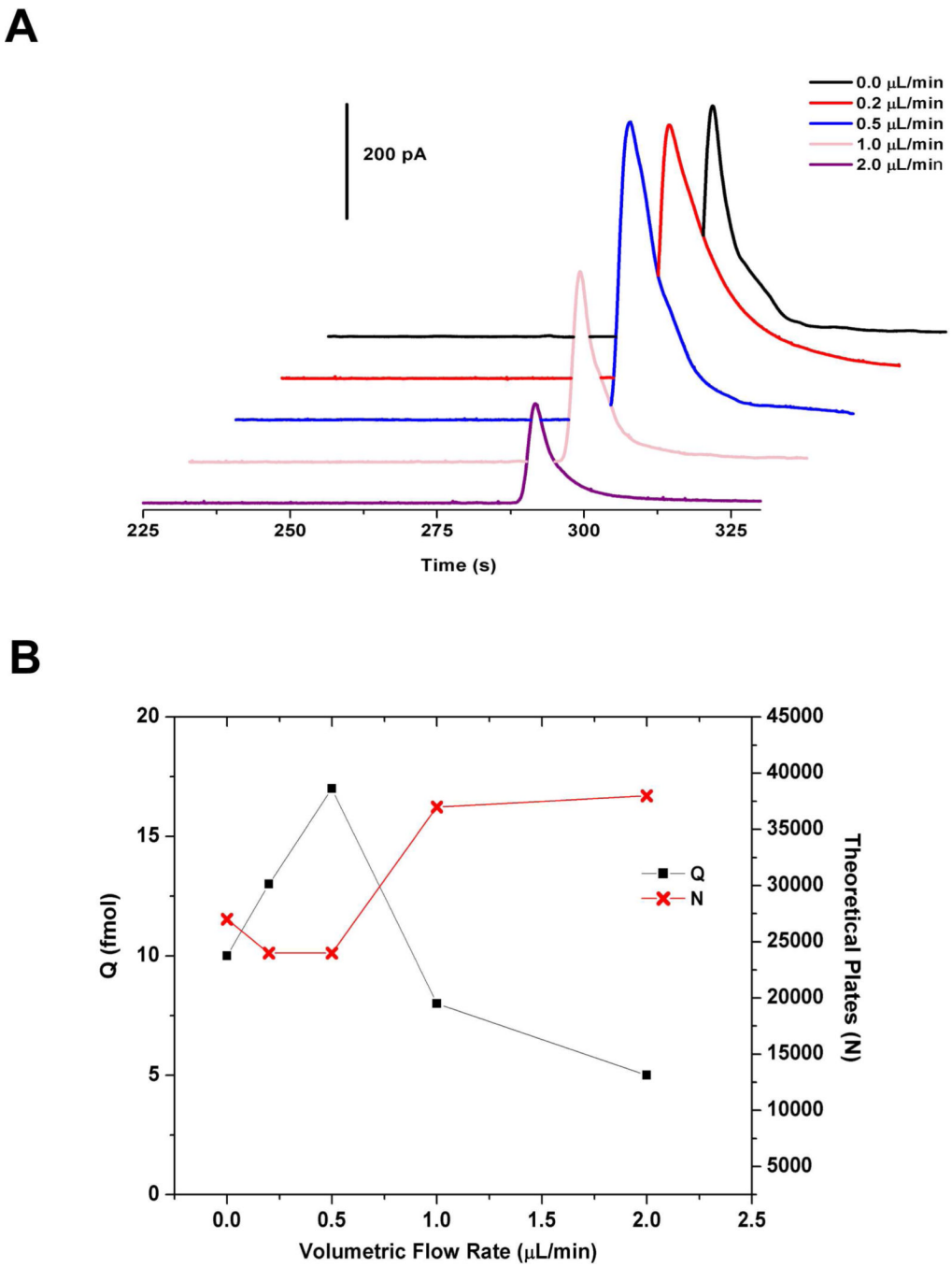

Figure 3.

Effect of volumetric flow rate through lysis channels on end-column electrochemical detection. A plug of 100 μM CAT solution was injected onto the capillary and run at 333 V/cm. Lysis buffer (50 mM TES/ 5%(w/v) SDS/ pH 7.4) was flowed through at varying volumetric flow rates. (A) Series of electropherograms for the detection of CAT at varying flow rates from 0 −2 μL/min. (B) Plot quantifying detection of CAT in terms of amount (Q) and separation efficiency (N) for the data in part A. Error bars omitted for clarity. Standard deviation of the mean listed in Table 1.

NIH-PA Author Manuscript

NIH-PA Author Manuscript

NIH-PA Author Manuscript

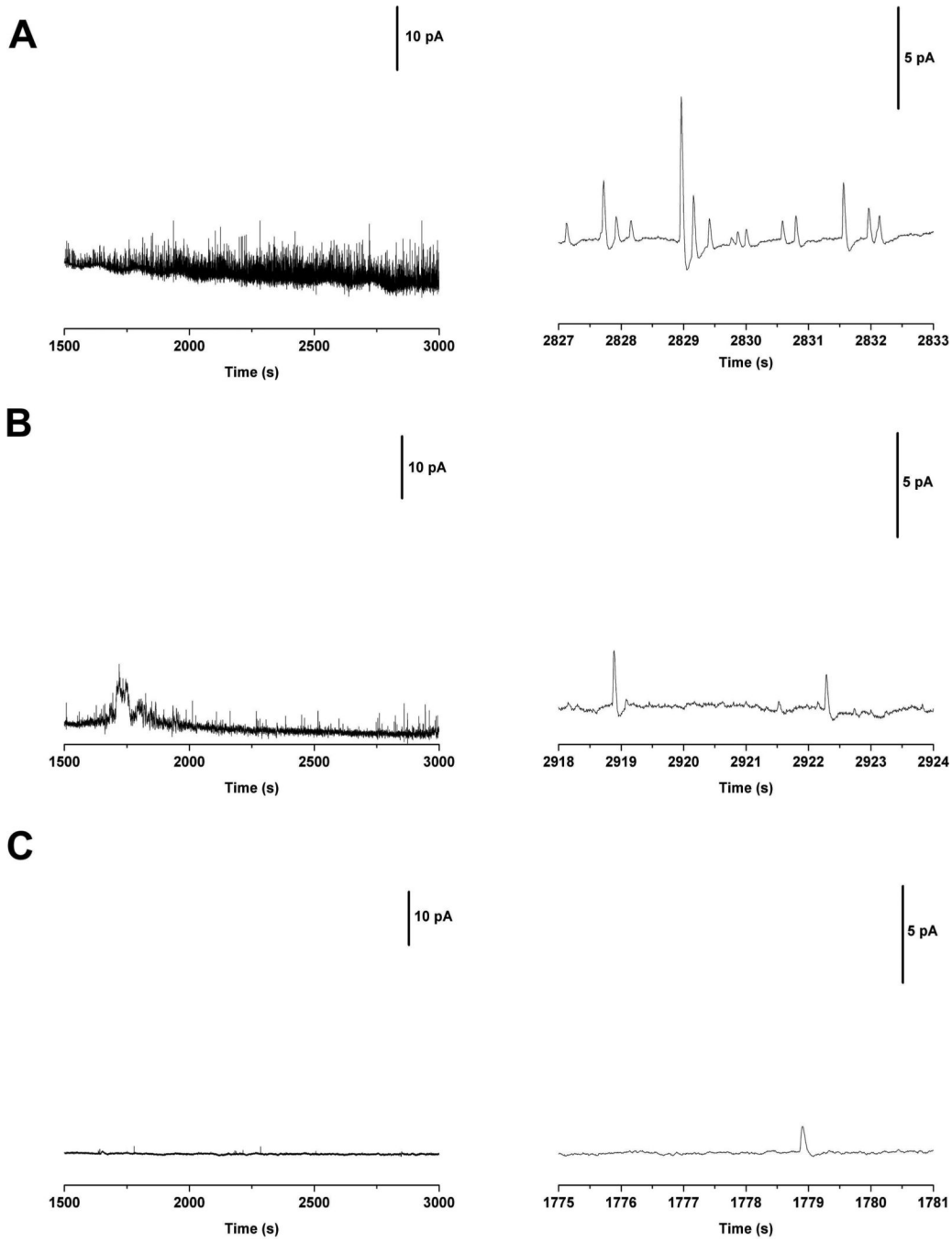

Figure 4.

Representative electropherograms for the end-column lysis and detection of liposomes. Liposomes injected for 20 s at 111 V/cm and run at 333 V/cm. Individual peaks are shown in the expanded view to the right. (A) Liposomes loaded with 150 mM DA. (B) A ten-fold dilution of the liposome suspension injected in part A. (C) Electropherogram of control liposomes that were loaded with buffer only (no DA).

NIH-PA Author Manuscript
NIH-PA Author Manuscript
NIH-PA Author Manuscript

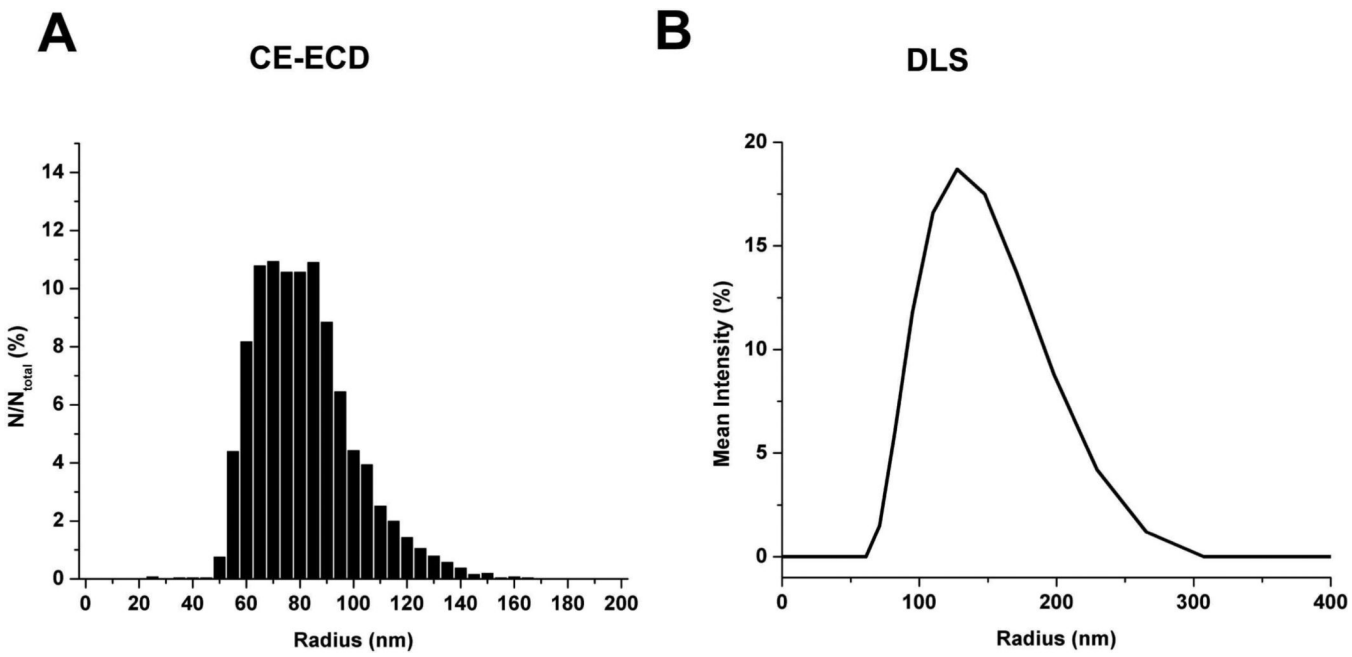

Figure 5.
Plot of the normalized frequency histogram describing the radius size distribution based on the internalized volume of dopamine detected from (A) CE-ECD and (B) DLS experiments for liposomes loaded with 150 mM DA. Average radii and standard deviation listed in Table 2.

NIH-PA Author Manuscript
NIH-PA Author Manuscript
NIH-PA Author Manuscript

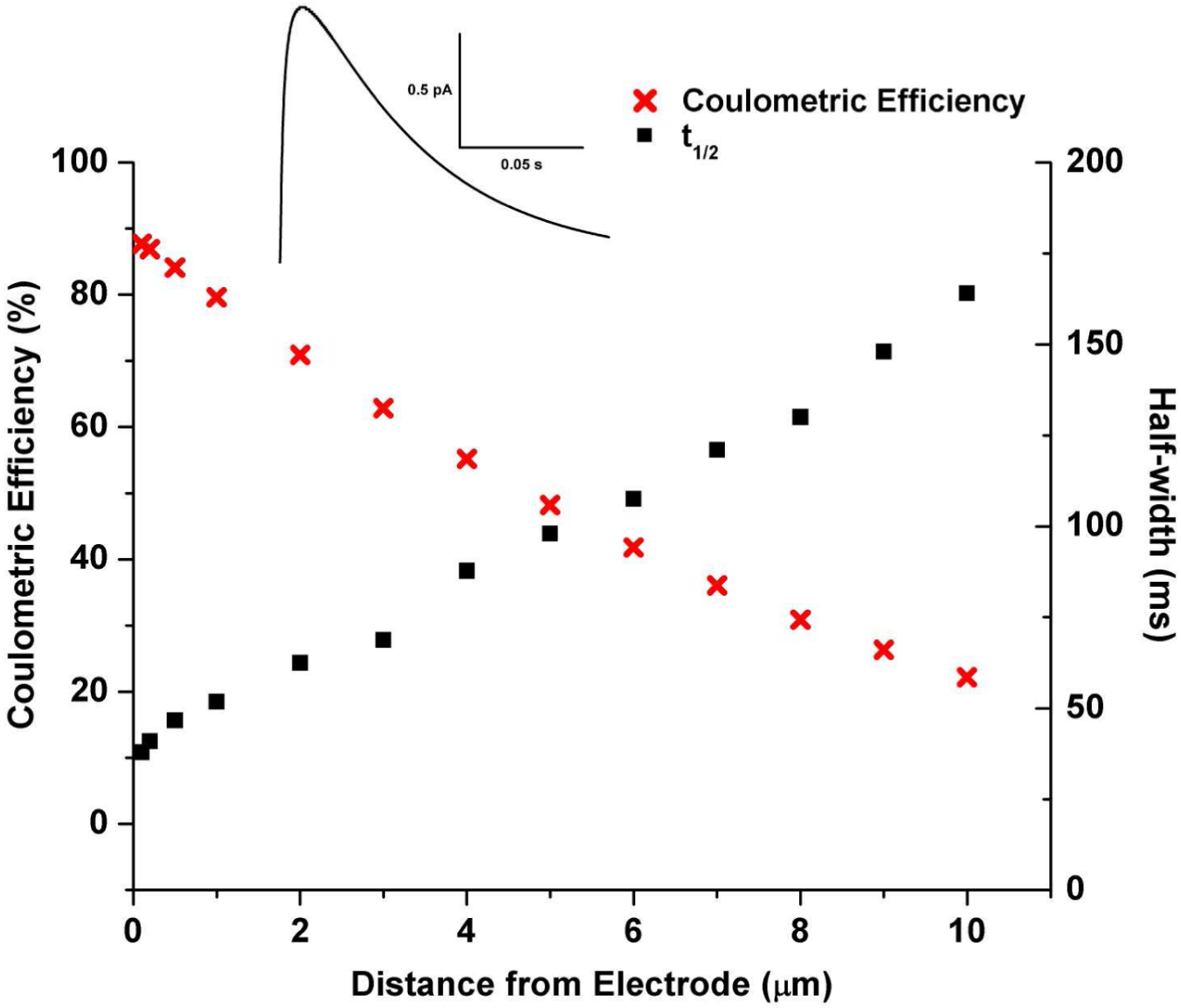

Figure 6.

Plot of simulated data for the half-width and coulometric efficiency for detection of dopamine following liposome lysis. Inset: resultant amperometric trace for a liposome filled with 150 mM DA, having a diameter of 200 nm, and lysing 0.25 μm away from the electrode. Distances are measured to the closest edge of the liposome in relation to the electrode.

NIH-PA Author Manuscript NIH-PA Author Manuscript NIH-PA Author Manuscript

Table 1

Effect of Sheath-Flow Rate on Detection of 100 μM Catechol Solution Eluting from Separation Capillary.

Sheath-Flow Rate (μL/min)	Amplitude (pA)	Amount (fmol)	Coulometric Efficiency (%)	Theoretical Plates (N)	LOD (μM)
0.0	390 ± 15	9.5 ± 1.0	19 ± 2	26000 ± 2600	0.57 ± 0.02
0.2	430 ± 46	12.8 ± 6.0	26 ± 14	24000 ± 1500	0.53 ± 0.05
0.5	480 ± 110	17.2 ± 6.1	36 ± 13	24000 ± 18000	0.50 ± 0.13
1.0	390 ± 170	7.8 ± 3.3	16 ± 6	37000 ± 12000	0.66 ± 0.27
2.0	250 ± 65	4.5 ±1.0	9 ± 2	38000 ± 13000	0.95 ± 0.27

n = 3. Error is the standard deviation of the mean.

NIH-PA Author Manuscript
NIH-PA Author Manuscript
NIH-PA Author Manuscript

Table 2

Liposome Characterization from CE-ECD and DLS Analyses.

Sample	Number of Peaks	Amplitude (pA)	Half-width (ms)	Amount of DA (zmol)	Radius CE-ECD (nm)	Radius DLS (nm)
150 mM DA Liposomes	2670	1.4 ± 0.9	42.2 ± 17.4	367 ± 289	79.3 ±18.4	115 ± 36
150 mM DA Liposomes Diluted	140	1.2 ± 0.7	27.2 ± 2.8	185 ±108	64.5 ±12.0	115 ± 36
Control Liposomes*	4	0.7 ± 0.3	62.0 ± 3.6	~	~	150 ± 48

*No DA present in this sample. Error is the standard deviation of the mean.